

Clinical utility of the normalized apparent diffusion coefficient for preoperative evaluation of the aggressiveness of prostate cancer

Ryo Itatani · Tomohiro Namimoto · Akira Yoshimura · Kazuhiro Katahira · Seiichiro Noda · Nobuyuki Toyonari · Kosuke Kitani · Yasuyuki Hamada · Mitsuhiko Kitaoka · Yasuyuki Yamashita

Received: 11 July 2014 / Accepted: 3 October 2014 / Published online: 17 October 2014
© Japan Radiological Society 2014

Abstract

Purpose Normalization of the apparent diffusion coefficient (ADC) may overcome ADC variability attributable to different patient and/or technical factors. The purpose of this study was to compare the efficacy of ADC and the normalized ADC (nADC) for differentiating between prostate cancer with a Gleason score (GS) = 6 and GS > 6 and to identify an optimum reference for nADC calculations.

Materials and methods Our study population comprised 58 patients who underwent diffusion-weighted MRI followed by radical prostatectomy. The nADC of the prostate cancer was calculated as ADC (cancer)/ADC (reference) by using the obturator internus muscle, urine in the bladder, and a 20-ml saline bottle placed on the groin as references. We performed receiver operating characteristic (ROC) analysis to identify the optimum reference for nADC calculations.

Results To differentiate between GS = 6 and GS > 6 prostate cancer, the area under the ROC curve of the nADC obtained with a saline bottle as reference was best (0.85) and significantly better than the area under the ADC ROC curve (0.71).

Conclusions nADC is superior to ADC for estimating the aggressiveness of prostate cancer. It is a noninvasive technique that aids in the selection of appropriate treatments.

Keywords Prostate cancer · Gleason score · Normalized ADC

Introduction

Prostate cancer is the most common cancer in Western men; among malignancies its incidence is the highest and its mortality is third highest [1]. As the range of prostate cancer varies from indolent to highly aggressive, accurate stratification of aggressiveness is essential. Treatment selection is based on serum prostate-specific antigen (PSA) level, digital rectal examination (DRE), and histopathological findings of transrectal ultrasonography (TRUS)-guided biopsy. On the basis of the likelihood of tumor spread and recurrence, localized prostate cancer is stratified as low, intermediate, and high-risk [2]. The Gleason score (GS) is the most commonly accepted and widely used value for evaluating the aggressiveness of prostate cancer. ESUR prostate MR guidelines 2012 [2] classify GS = 6 as low-risk and GS > 6 as intermediate-to-high risk prostate cancer. To avoid serious side effects, low-risk prostate cancer must be diagnosed correctly to prevent unnecessary biopsies or such whole-gland treatments as radical prostatectomy and radiation therapy [3].

R. Itatani (✉) · T. Namimoto · Y. Yamashita
Department of Diagnostic Radiology, Graduate School of
Medical Sciences, Kumamoto University, 1-1-1, Honjo,
Kumamoto 860-8556, Japan
e-mail: banguliao@gmail.com

R. Itatani · A. Yoshimura · K. Katahira · S. Noda · N. Toyonari
Department of Radiology, Kumamoto Chuo Hospital,
1-5-1, Tainoshima, Kumamoto 862-0965, Japan

K. Kitani · Y. Hamada
Department of Urology, Kumamoto Chuo Hospital,
1-5-1, Tainoshima, Kumamoto 862-0965, Japan

M. Kitaoka
Department of Pathology, Kumamoto Chuo Hospital,
1-5-1, Tainoshima, Kumamoto 862-0965, Japan

Diffusion-weighted imaging (DWI) is a functional imaging technique that yields qualitative and quantitative information on water molecules in tissues. The apparent diffusion coefficient (ADC) is lower for malignancies with greater cell density and space. Prostate MRI studies have shown that the ADC correlates negatively with the GS [4, 5]. However, comparison of ADC values obtained in different studies is difficult, because they vary with the equipment used, the scanning procedures, the b values, and the age and body temperature of patients [6–13]. The normalized ADC (nADC), calculated by use of the equation $\text{ADC (lesion)}/\text{ADC (reference)}$, can be used to overcome potential limitations. Determination of the nADC may be necessary because normalization reduces ADC variability attributable to different patient and/or technical factors; it has been useful in evaluation of the brain, liver, pancreas, and bone [14–17]. With regard to the pelvic lesion, it has been reported that the nADC is superior to the ADC for estimating the histological grade of bladder carcinoma [18]. The nADC can therefore be useful for reducing the variability of ADC for estimating prostate cancer aggressiveness.

As far as we are aware, however, the clinical applicability of the nADC to prostate cancer has not been sufficiently investigated. The objective of this study was to compare the efficacy of the ADC and the nADC in differentiating between $\text{GS} = 6$ and $\text{GS} > 6$ prostate cancer and to identify the optimum reference for nADC calculations.

Materials and methods

This prospective study received institutional review board approval; informed consent was obtained from all patients prior to their participation.

Patients

Our study included 70 consecutive patients who underwent radical prostatectomy for pathologically confirmed prostate cancer at our institution between January 2013 and February 2014; all had undergone 3T prostate MRI (including DWI) before prostatectomy and all fulfilled our inclusion criteria. We excluded 12 patients who had received hormone treatment before prostatectomy. Consequently, 58 patients (ranging in age from 58 to 81 years, mean 70.7 ± 6.4 years) were included. All patients underwent TRUS-guided biopsy before prostatectomy and 48 underwent biopsy after MRI. The other 10 patients underwent TRUS-guided biopsy before MRI, however the interval between biopsy and MRI was at least 6 weeks to prevent biopsy-related hemorrhage [19]. The interval between MRI

study and radical prostatectomy was 45.9 ± 35.0 days (range 9–215 days, median 35 days). The preoperative PSA level ranged from 4.4 to 61.1 ng/ml (mean 10.9 ± 10.5 ng/ml, median 7.6 ng/ml).

MRI

For the MRI studies on our 3T scanner (Ingenia; Philips Medical Systems) we used a 32-channel cardiac SENSE coil. Although patients were not fasting they reduced their diet to approximately 1/3 of normal. If the images were poor because of peristalsis we intravenously injected 20 mg hyoscinebutylbromide (Buscopan; Boehringer, Ingelheim, Germany) and re-started the examination immediately. Axial T2-weighted images, coronal T2-weighted images with fat suppression (FS), axial DWI with two different b values (0 and 1000 s/mm^2), and ADC maps using the two b values were obtained. The imaging settings for each sequence are shown in Table 1. We affixed a plastic bottle containing 20 ml saline to each patient's groin for ADC interpretation. In the examination room we kept the saline bottle at 23°C to minimize temperature changes because the ADC depends on body temperature [20]. To prevent contamination, disposable bottles were used.

Pathology

All patients underwent radical prostatectomy after MRI. Each prostatectomy specimen was step-sectioned into 4-mm slices. In routine pathology studies cancer foci were outlined in ink on step-section slices of the prostate. The pathology results were reported by use of the GS system. For radiology–pathology correlation studies, a region was recorded as positive if it contained a tumor with a cross-

Table 1 Imaging settings used

Setting	T2WI	T2WI-FS	DWI ($b = 0, 1000 \text{ s/mm}^2$)
Acquisition plane	Transverse	Coronal	Transverse
TR (ms)	7000	2907	5584
TE (ms)	100	80	53
FOV (mm)	200	200	350
Matrix	288	256	160
Slice thickness/gap (mm)	4/0.4	4/0.4	4/0.4
FA ($^\circ$)	90	90	90
NSA	1	1	3
ETL/EPI factor	9	23	67
Acquisition time (s)	189	64	178

EPI echo-planar imaging, ETL echo train length, FA flip angle, FOV field of view, FS fat saturation, NSA number of signals averaged, TE echo time, TR repetition time, TSE turbo spin echo

sectional area greater than 4 mm in diameter (equivalent to a 0.13 cm² area) [21–23]. Markers used for alignment of MR images with histologic slices included the morphologic features of the peripheral zone, transitional zone, apex, midgland, and base of the prostate, and cysts, calcifications, the verumontanum, and the urethra [24, 25]. Each patient's GS was recorded by a board-certified pathologist with 34 years of experience in interpreting prostate pathology.

Image interpretation

A board-certified radiologist with seven years of experience interpreting prostate MR images matched the step-sectioned pathologic slices with the corresponding T2-weighted images and ADC maps. Regions of interest (ROIs), as large as possible, were drawn manually in the center of the visible pathologically-positive area with the lowest signal. If a pathologic map and a corresponding ADC map contained more than one tumor, the dominant lesion corresponding each patient's GS with the lowest mean ADC value was used. In the selection of the ROIs on the ADC maps, the tumor margin, prostate capsule, neurovascular bundles, and urethra were excluded. The mean ADC values were automatically calculated on a picture archiving and communication systems (PACS) workstation (EV Insight 2.10.8.81; PSP, Tokyo, Japan): the actual ROI area ranged from 18 to 251 mm². To select the optimum reference for the nADC calculations, ADC values were also obtained from the obturator internus muscle, urine in the bladder lumen, and the 20-ml saline bottle placed on the groin. Reference ROIs were at least 20 mm²; they were placed in areas as homogenous as possible and visible artifacts were carefully excluded (Fig. 1). The nADC was calculated by use of the equation ADC (prostate cancer)/ADC (reference). The nADC from the references, i.e. the obturator internus muscle, urine in the bladder, and the saline bottle were identified as nADCM, nADCu, and nADCs, respectively. The best cutoff ADC and nADC for identification of prostate cancer with a GS = 6 from GS > 6 were calculated. To investigate the effect of cancer location, ROC analysis was also performed for limited cases with peripheral zone prostate cancer.

Statistical analysis

Student's *t* test was used to compare the ADC and nADC values for GS = 6 and GS > 6 prostate cancer. The ADC and the nADC values obtained by use of the three references were compared with the GS of the radical prostatectomy specimens; receiver operating characteristic (ROC) analysis was performed to differentiate between GS = 6 and GS > 6 prostate cancer. The ROC curves were

drawn by use of computer software (MedCalca, version 9.3.1; MedCalc Software, Mariakerke, Belgium) and the areas under the ROC curves (AUC) were compared. Statistical significance was defined as $p < 0.05$.

Results

On the basis of our pathology findings for the total of 58 prostatectomies, 7 patients (12 %) had GS = 6 (3 + 3) prostate cancer, and the other 51 (88 %) had GS > 6 prostate cancer: 3 + 4, $n = 10$; 4 + 3, $n = 31$; 4 + 4, $n = 6$; 4 + 5, $n = 4$. For the dominant lesion of prostate cancer, 36 were peripheral zone and 21 were transitional zone. T stages for all patients were: T2a, $n = 17$; T2b, $n = 2$; T2c, $n = 34$; T3b, $n = 5$. ADC and nADC values for GS = 6 cancers were higher than those for GS > 6 cancers. Differences among ADC, nADCu, and nADCs values were significant (Table 2).

ROC analysis showed that the AUC for ADC, nADCM, nADCu, and nADCs were 0.711, 0.703, 0.762 and 0.846, respectively (Fig. 2). The AUC for nADCs was significantly larger than for ADC for differentiation between GS = 6 and GS > 6 prostate cancer ($p = 0.024$). The best cutoff nADCs for identification of prostate cancer with GS = 6 was 0.37, with 74.5 % sensitivity and 85.7 % specificity, whereas the best cutoff ADC was 1.1 with 82.4 % sensitivity and 57.1 % specificity. The scatter diagrams for ADC and nADC are shown in Fig. 3.

With regard to ROC analysis for peripheral zone prostate cancer ($n = 36$ including six GS = 6 prostate cancer), AUC for ADC, nADCM, nADCu, and nADCs were 0.775, 0.678, 0.778 and 0.856, respectively. The AUC excluding nADCM were better than for the ROC analysis including all 58 cases; there were, however, no significant differences between ADC and each nADC for differentiating between GS = 6 and GS > 6 prostate cancer.

Discussion

Although ADC values correlate negatively with tumor aggressiveness [4, 5], their low comparability among studies is a serious problem when the ADC value is used to evaluate cancer aggressiveness. The lack of standardized DWI procedures reduces the reliability of ADC comparisons among studies because the equipment, vendors, coils, pulse sequences, scanner settings, and magnetic susceptibility artifacts are different. These differences can result in inter-study ADC differences of 5–15 % [6, 13, 26–28]. We report that the AUC for nADCu and nADCs was higher than for ADC and that the AUC for nADCs was significantly higher than that for ADC for differentiation between

Fig. 1 ADC measurement of prostate cancer: axial T2WI (a) and axial ADC map at the same slice level (b), at the level of the bladder (c), and at the level of the groin (d). The white arrow indicates prostate cancer in the left peripheral zone (b). ROIs (yellow circles) were placed on the obturator internus muscles (b), urine in the bladder (c), and the 20-ml saline bottle placed on the groin (d)

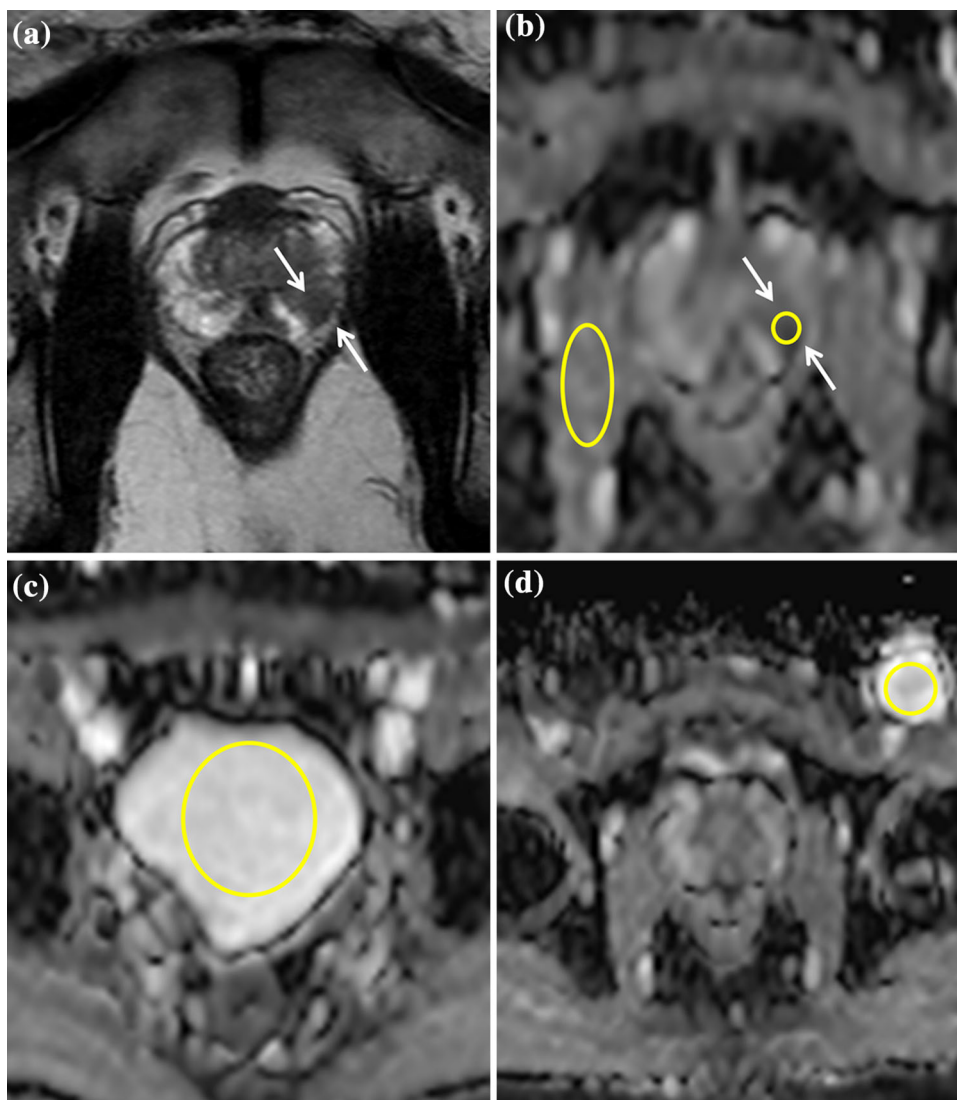


Table 2 Comparison of ADC and nADC values for prostate cancer

	Prostate cancer with GS = 6	Prostate cancer with GS > 6	<i>p</i> value
ADC	1.14 ± 0.22	0.96 ± 0.15	<0.01
nADC _m	0.97 ± 0.20	0.84 ± 0.17	0.058
nADC _u	0.44 ± 0.10	0.33 ± 0.051	<0.01
nADC _s	0.40 ± 0.083	0.33 ± 0.053	<0.01

GS = 6 and GSA > 6 prostate cancer. This observation suggests that the nADC is superior to the ADC for estimating the aggressiveness of prostate cancer and that it can be useful for the selection of appropriate treatments.

We attribute our finding that use of saline as reference yielded the best nADC to the greater homogeneity of saline

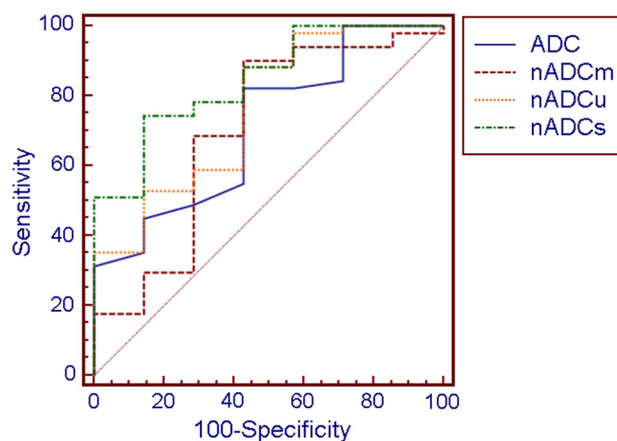
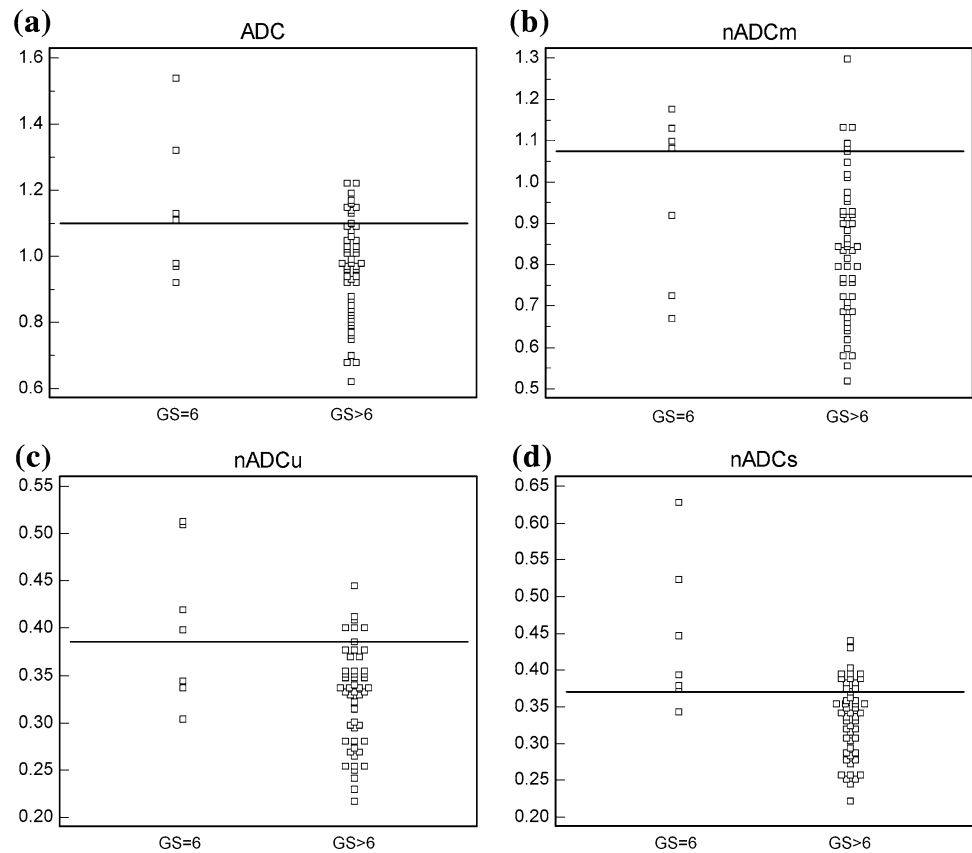


Fig. 2 Results from ROC analysis for differentiation between GS = 6 and GS > 6 prostate cancer

Fig. 3 Scatter diagrams for differentiation between GS = 6 and GS > 6 prostate cancer; **a** ADC, **b** nADCm, **c** nADCu, and **d** nADCs



over urine. Wang et al. [18] demonstrated that the nADC using urine in the bladder lumen as a reference is best for estimating the histological grade of vesical urothelial carcinoma. Although they used different materials and methods, their results were consistent with ours with regard to the superiority of the nADC. We suggest that using reference materials similar to water can aid identification of the aggressiveness of pelvic cancers. In contrast, the AUC of the nADCm was equivalent to that of the ADC and the AUC of the nADCu and nADCs was better than of the ADC, possibly because of individual variations in the amount of muscle. Although the results in a previous report [18] were different from ours with regard to the utility of the nADC with muscles as reference, they were consistent with our finding that the nADC using urine in the bladder yielded a better AUC. Nonetheless, we consider urine or saline to be a better reference for the nADC than muscles, because inter-patient variations may be smaller and we believe it is the most important factor in the greater ability observed for nADC for discrimination between the aggressiveness of prostate cancer. Although saline was the best reference for the nADC in our study, in the clinical setting, urine in the bladder may be an alternative reference.

Interpretation of ADC for patients with prostate cancer undergoing MRI has been discussed. Litjens et al. [29]

reported significant inter-patient variation ($1.2\text{--}2.0 \times 10^{-3} \text{ mm}^2/\text{s}$) of peripheral zone ADCs which affected predictability of the aggressiveness of prostate cancer. According to Jacobs et al. [20], in-vivo (37°C) ADC measurements in the same prostate region of the same individual were significantly (36–48 %) higher than in-vitro (23°C) measurements. To minimize such ADC variations, all of our patients were scanned on the same 3T instrument using identical coils, pulse sequences, and scanner settings, and the temperature of the saline bottle was maintained at 23°C . In previous studies with a 3T scanner that used ADC of $b = 0$ and $b = 1000 \text{ s}/\text{mm}^2$, ADC values for GS = 6 prostate cancer varied from 1.19 to $1.25 \times 10^{-3} \text{ mm}^2/\text{s}$ [6, 30, 31]. Our values were slightly lower ($1.14 \times 10^{-3} \text{ mm}^2/\text{s}$), suggesting that there are variations in the ADC of prostate cancer even when the same MRI settings and b values are used. Lim et al. [32] reported that adding an ADC map to T2-weighted images can improve the diagnostic performance of MRI in the detection of prostate cancer. They emphasized that, as in brain imaging, the nADC should be used to reduce ADC variability on prostate MRI scans. We support their suggestion and our findings provide a clue for evaluation of prostate cancer aggressiveness using the nADC. Nonetheless the clinical application of nADC has not yet been sufficiently investigated; further multi-center prospective studies should

therefore be conducted to determine whether nADC really can equalize inter-study ADC variability.

Our study has some limitations:

- First, there is the issue of selection bias, because all of our patients underwent radical prostatectomy, thereby excluding patients with more aggressive prostate cancer.
- Second, the temperature of the saline bottle placed on the patients' groin may rise, because of their body temperature, during the MRI study. Nevertheless, because saline is more homogenous than urine in the bladder, its use as a reference yields more reliable results.
- Third, we did not investigate cancer detection performance in this study. However, as previous report [33] showed good performance of cancer detection using T2WI and DWI at 3T (AUC = 0.78–0.79). Moreover the authors demonstrated that DWI correlated significantly with prostate cancer aggressiveness. Because our results are in agreement with theirs, nADC may provide better clinical information about tumor aggressiveness and cancer detection.
- Fourth, there is an inherent limitation in correlating imaging and histologic findings on a section-by-section basis, because the angle of the histologic slices and the MRI scans may be different and prostate tissue tends to shrink during fixing.

In conclusion, the nADC is superior to the ADC for estimating the aggressiveness of prostate cancer and is a noninvasive technique that aids in the selection of appropriate treatments for patients with prostate cancer.

Conflict of interest The authors declare that they have no conflict of interest.

References

1. Jemal A, Bray F, Center MM, et al. Global cancer statistics. *CA Cancer J Clin*. 2011;61(2):69–90.
2. Barentsz JO, Richenberg J, Clements R, et al. ESUR prostate MR guidelines 2012. *Eur Radiol*. 2012;22(4):746–57.
3. Itatani R, Namimoto T, Kajihara H, et al. Triage of low-risk prostate cancer patients with PSA levels 10 ng/ml or less: comparison of apparent diffusion coefficient value and transrectal ultrasound-guided target biopsy. *AJR Am J Roentgenol*. 2014; 202(5):1051–7.
4. Hambrock T, Somford DM, Huisman HJ, et al. Relationship between apparent diffusion coefficients at 3.0-T MR imaging and Gleason grade in peripheral zone prostate cancer. *Radiology*. 2011;259(2):453–61.
5. Turkbey B, Shah VP, Pang Y, et al. Is apparent diffusion coefficient associated with clinical risk scores for prostate cancers that are visible on 3-T MR images? *Radiology*. 2011;258(2):488–95.
6. Kitajima K, Takahashi S, Ueno Y, et al. Clinical utility of apparent diffusion coefficient values obtained using high *b*-value when diagnosing prostate cancer using 3 tesla MRI: comparison between ultra-high *b*-value (2000 s/mm²) and standard high *b*-value (1000 s/mm²). *J Magn Reson Imaging*. 2012;36(1):198–205.
7. Hoehn-Berlage M, Eis M, Schmitz B. Regional and directional anisotropy of apparent diffusion coefficient in rat brain. *NMR Biomed*. 1999;12(1):45–50.
8. DeLano MC, Cooper TG, Siebert JE, et al. High-*b*-value diffusion-weighted MR imaging of adult brain: image contrast and apparent diffusion coefficient map features. *AJNR Am J Neuro-radiol*. 2000;21(10):1830–6.
9. Mulkern RV, Barnes AS, Haker SJ, et al. Biexponential characterization of prostate tissue water diffusion decay curves over an extended *b*-factor range. *Magn Reson Imaging*. 2006;24(5):563–8.
10. Thoeny HC, De Keyzer F, Oyen RH, et al. Diffusion-weighted MR imaging of kidneys in healthy volunteers and patients with parenchymal diseases: initial experience. *Radiology*. 2005;235(3):911–7.
11. Bilgili Y, Unal B. Effect of region of interest on interobserver variance in apparent diffusion coefficient measures. *AJNR Am J Neuroradiol*. 2004;25(1):108–11.
12. Ulug AM, Beauchamp N Jr, Bryan RN, et al. Absolute quantitation of diffusion constants in human stroke. *Stroke*. 1997;28(3): 483–90.
13. Tamada T, Sone T, Jo Y, et al. Apparent diffusion coefficient values in peripheral and transition zones of the prostate: comparison between normal and malignant prostatic tissues and correlation with histologic grade. *J Magn Reson Imaging*. 2008;28(3):720–6.
14. Oh J, Henry RG, Pirzkall A, et al. Survival analysis in patients with glioblastoma multiforme: predictive value of choline-to-*N*-acetylaspartate index, apparent diffusion coefficient, and relative cerebral blood volume. *J Magn Reson Imaging*. 2004;19(5): 546–54.
15. Do RK, Chandarana H, Felker E, et al. Diagnosis of liver fibrosis and cirrhosis with diffusion-weighted imaging: value of normalized apparent diffusion coefficient using the spleen as reference organ. *AJR Am J Roentgenol*. 2010;195(3):671–6.
16. Barral M, Sebbag-Sfez D, Hoeffel C, et al. Characterization of focal pancreatic lesions using normalized apparent diffusion coefficient at 1.5-Tesla: preliminary experience. *Diagn Interv Imaging*. 2013;94(6):619–27.
17. Park SO, Kim JK, Kim KA, et al. Relative apparent diffusion coefficient: determination of reference site and validation of benefit for detecting metastatic lymph nodes in uterine cervical cancer. *J Magn Reson Imaging*. 2009;29(2):383–90.
18. Wang HJ, Pui MH, Guo Y, et al. Value of normalized apparent diffusion coefficient for estimating histological grade of vesical urothelial carcinoma. *Clin Radiol*. 2014;69(7):727–31.
19. Wang L, Mazaheri Y, Zhang J, et al. Assessment of biologic aggressiveness of prostate cancer: correlation of MR signal intensity with Gleason grade after radical prostatectomy. *Radiology*. 2008;246(1):168–76.
20. Jacobs MA, Ouwkerk R, Petrowski K, et al. Diffusion-weighted imaging with apparent diffusion coefficient mapping and spectroscopy in prostate cancer. *Top Magn Reson Imaging*. 2008; 19(6):261–72.
21. Haider MA, van der Kwast TH, Tanguay J, et al. Combined T2-weighted and diffusion-weighted MRI for localization of prostate cancer. *AJR Am J Roentgenol*. 2007;189(2):323–8.
22. Kikuchi E, Scardino PT, Wheeler TM, et al. Is tumor volume an independent prognostic factor in clinically localized prostate cancer? *J Urol*. 2004;172(2):508–11.
23. Ohori M, Wheeler TM, Dunn JK, et al. The pathological features and prognosis of prostate cancer detectable with current diagnostic tests. *J Urol*. 1994;152(5 Pt 2):1714–20.
24. Hosseinzadeh K, Schwarz SD. Endorectal diffusion-weighted imaging in prostate cancer to differentiate malignant and benign peripheral zone tissue. *J Magn Reson Imaging*. 2004;20(4):654–61.

25. Zakian KL, Sircar K, Hricak H, et al. Correlation of proton MR spectroscopic imaging with gleason score based on step-section pathologic analysis after radical prostatectomy. *Radiology*. 2005;234(3):804–14.
26. Braithwaite AC, Dale BM, Boll DT, et al. Short- and midterm reproducibility of apparent diffusion coefficient measurements at 3.0-T diffusion-weighted imaging of the abdomen. *Radiology*. 2009;250(2):459–65.
27. Sasaki M, Yamada K, Watanabe Y, et al. Variability in absolute apparent diffusion coefficient values across different platforms may be substantial: a multivendor, multi-institutional comparison study. *Radiology*. 2008;249(2):624–30.
28. Koh DM, Blackledge M, Collins DJ, et al. Reproducibility and changes in the apparent diffusion coefficients of solid tumours treated with combretastatin A4 phosphate and bevacizumab in a two-centre phase I clinical trial. *Eur Radiol*. 2009;19(11):2728–38.
29. Litjens GJ, Hambrock T, Hulsbergen-van de Kaa C, et al. Inter-patient variation in normal peripheral zone apparent diffusion coefficient: effect on the prediction of prostate cancer aggressiveness. *Radiology*. 2012;265(1):260–6.
30. Kim CK, Park BK, Kim B. High-*b*-value diffusion-weighted imaging at 3T to detect prostate cancer: comparisons between *b* values of 1,000 and 2,000 s/mm². *AJR Am J Roentgenol*. 2010;194(1):W33–7.
31. Vargas HA, Akin O, Franiel T, et al. Diffusion-weighted endorectal MR imaging at 3 T for prostate cancer: tumor detection and assessment of aggressiveness. *Radiology*. 2011;259(3):775–84.
32. Lim HK, Kim JK, Kim KA, et al. Prostate cancer: apparent diffusion coefficient map with T2-weighted images for detection—a multireader study. *Radiology*. 2009;250(1):145–51.
33. Turkbey B, Pinto PA, Mani H, et al. Prostate cancer: value of multiparametric MR imaging at 3 T for detection—histopathologic correlation. *Radiology*. 2010;255(1):89–99.